Journal of Medicinal Chemistry

Article

pubs.acs.org/jmc

Solubility-Driven Optimization of Phosphodiesterase-4 Inhibitors Leading to a Clinical Candidate

Neil J. Press,*[,†] Roger J. Taylor,[†] Joseph D. Fullerton, Pamela Tranter,[†] Clive McCarthy, Thomas H. Keller, Nicola Arnold, David Beer,[∥] Lyndon Brown, Robert Cheung, Julie Christie, Alastair Denholm, Sandra Haberthuer, Julia D. I. Hatto,[†] Mark Keenan, Mark K. Mercer, Helen Oakman,[†] Helene Sahri, Andrew R. Tuffnell, Morris Tweed, John W. Tyler,[†] Trixie Wagner,[‡] John R. Fozard,[§] and Alexandre Trifilieff[‡]

[†]Novartis Institutes for Biomedical Research, Wimblehurst Road, Horsham, West Sussex RH12 5AB, U.K.

[‡]Novartis Institutes for Biomedical Research, Lichtstrasse 35, CH-4056 Basel, Switzerland

[§]Novartis Distinguished Scientist, Novartis Institutes for Biomedical Research, Lichtstrasse 35, CH-4056 Basel, Switzerland

[∥]Novartis Institute for Tropical Diseases, 10 Biopolis Road, 05-01 Chromos, 138670 Singapore

Supporting Information

ABSTRACT: The solubility-driven optimization of a series of 1,7-napthyridine phosphodiesterase-4 inhibitors is described. Directed structural changes resulted in increased aqueous solubility, enabling superior pharmacokinetic properties with retention of PDE4 inhibition. A range of potent and orally bioavailable compounds with good in vivo efficacy in animal models of inflammation and reduced emetic potential compared to previously described drugs were synthesized. Compound **2d** was taken forward as a clinical candidate for the treatment of COPD.

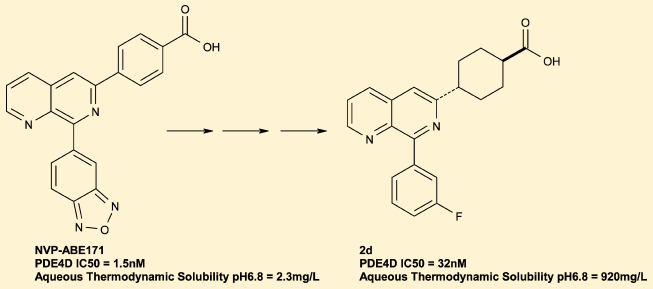

INTRODUCTION

Phosphodiesterase-4 (PDE4) has been an important therapeutic target for some time, with a strong rationale for the potential of an inhibitor to be of therapeutic benefit in a wide range of disease states.[1,2] PDE4 is mainly expressed in inflammatory cells, where it catalyzes the degradation of cAMP to AMP. Inhibiting this process is expected to result in an accumulation of intracellular cAMP, which is known to lead to a broad range of anti-inflammatory effects, making this an attractive target for inter alia respiratory diseases such as asthma and chronic obstructive pulmonary disease (COPD).[3−5] Indeed, drugs such as roflumilast and cilomilast have proven to be clinically beneficial in these disorders.[6] One reason why so many published PDE4 inhibitors have failed so far to be progressed to market is their propensity to show a high side effect profile (initially nausea and emesis) and low therapeutic index. While several theories have been published suggesting ways to design molecules in order to avoid side effects (ranging from selectively targeting a particular isoform such as PDE4B to avoiding the high affinity rolipram binding site (HARBS)), it is true to say that there is no current consensus as to the validity of any of these.[7a] Alternative approaches could utilize delivery methods focused on obtaining peripheral selectivity, thereby avoiding putative CNS-generated nausea effects, for example, by the introduction of hydrophilic moieties, or local administration by inhalation.[7b]

We have previously described the synthesis of a range of PDE4 inhibitors around the 1,7-naphthyridine scaffold. Primary among these was compound NVP-ABE171 (**4**, Figure 1), which

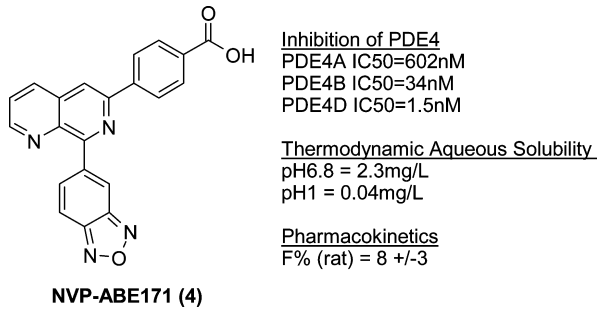

Figure 1. Structure and properties of **4**.

was shown to be a potent anti-inflammatory agent in in vivo models of inflammation.[8−10] Although **4** was efficacious when dosed orally in the inflammation model, the poor pharmacokinetics and low solubility of the compound precluded further development. The project therefore continued with the specific aim of producing a PDE4 inhibitor with improved solubility

Received: April 2, 2012
Published: August 13, 2012

Scheme 1. Synthetic Scheme for the Preparation of Key Intermediate 1

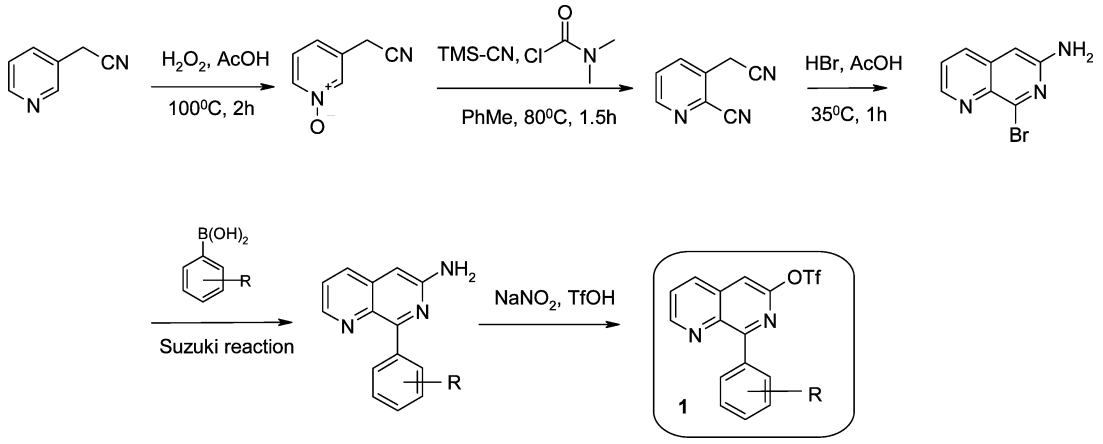

Scheme 2. Elaboration of Key Intermediate 1

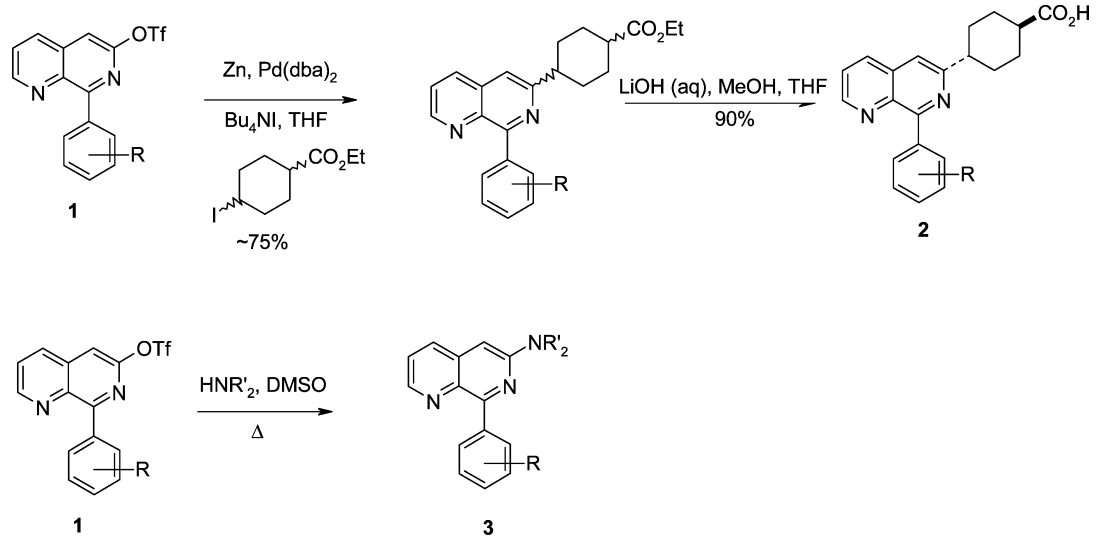

and pharmacokinetics. Furthermore, it was felt that a compound with a particularly reproducible and predictable pharmacokinetic profile (enabled by high solubility) would be of great benefit in this project, where we anticipated that the therapeutic index would be low.

RESULTS AND DISCUSSION

We decided to keep the 1,7-naphthyridine core scaffold and attempt to improve solubility by breaking up what we saw as the very flat, highly aromatic structure of **4**. We hypothesized that removal of two aromatic rings was feasible: the oxadiazole ring (replacing it with *m*-electron withdrawing groups) and the benzoic acid moiety (replacing, for example, with a cyclohexyl group). These changes were proposed in order to introduce a more three-dimensional morphology to the compound, the aim being to weaken the crystal structure of **4** and improve dissolution rate. We were keen to maintain the presence of the carboxylic acid in the molecule both as a handle for salt formation, and also with an aim to limiting the penetration of the compound into the central nervous system, it being considered that this would help to reduce the nausea/emesis side effect profile.

The synthesis of the compounds in two series (6-amino- or 6-carbo-substituted 1,7-naphthyridines) is shown in Schemes 1 and 2. Thus 6-amino-8-bromo-1,7-naphthyridine is synthesized in three steps from commercially available pyridine-3-ylacetonitrile. From this intermediate, Suzuki coupling proceeds smoothly at the 8-position to give a range of substituted aromatics, which were used as replacements for the benzoxadiazole moiety of **4** (Scheme 1). Diazotization followed by substitution with triflate gave key intermediate **1** (with various '*R*'), which we were able to elaborate at the 6-position either through Negishi coupling to form the carbocyclic series **2**, or through direct displacement to give the amino series 3 (Scheme 2). The former reaction is an elegant example of the coupling of a heteroaromatic triflate to an alkyzincate, allowing rapid access to a series of carbon-linked analogues. The cyclohexyl iodide was synthesized from the alcohol as a mixture of geometric isomers. However, the ratio of isomers was not important, as after the ester hydrolysis step the trans-stereochemistry was observed exclusively on the cyclohexyl ring; this geometry was proven by nuclear magnetic resonance analysis and by the X-ray structure determination of several analogues (see for example Figure 2).[11]

Table 1 contains the results of several representative compounds from each series in our PDE4 assays. Pleasingly, replacement of the benzoic acid moiety of **4** with either the saturated analogue or the piperidine analogue resulted in

dx.doi.org/10.1021/jm300459a | J. Med. Chem. 2012, 55, 7472−7479

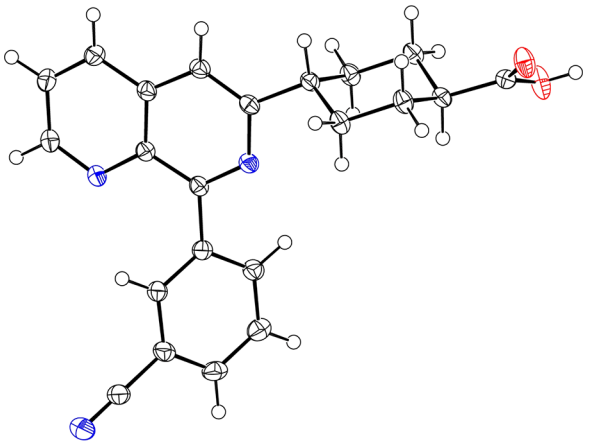

Figure 2. Structure of compound **2b** (R = CN) in the crystal, showing the trans-stereochemistry of the substituents at the cyclohexyl ring.[11]

compounds which were still inhibitors of the various PDE4 isoforms. The cyclohexyl series generally showed higher affinity across all isoforms than the piperidinyl analogues. As expected from our previous SAR knowledge, substitution on the 8-phenyl group with a *m*-electron withdrawing group generally led to good affinity at PDE4, with minor differences in rank order according to substituent in each series.

Also shown in Table 1 are results from an assay measuring inhibition of TNF-α release from stimulated human peripheral blood mononuclear cells (PBMCs); this is significant because it demonstrates that these acids are able to permeate the cell wall in order to act intracellularly. It is seen that the trend for the 6-cyclohexyl series to show highest inhibition of PDE4 activity is paralleled in this functional system. In this case, the difference between the two series is more obvious and led to the deprioritization of the piperidyl series due to the critical nature of achieving cellular activity (compare **2b** with **3b**, **2d** with **3d**, and **2f** with **3f**). This may be due to inherently lower affinity to the enzyme of the piperidinyl (**3**) series combined with a reduced cell permeability of that series (cLogP of series **3** compared with **2** is generally 1 order of magnitude lower, with a higher polar surface area). The cell penetration hypothesis was supported with passive diffusion permeability data from the parallel artificial membrane permeability assay (PAMPA, Table 1), which clearly shows poorer permeability for the piperidyl class (**3**) compared to cyclohexyl (**2**).

Crucially, these structural modifications led to a considerable and general increase in solubility compared to the highly unsaturated **4** (Table 1). We believe that the elimination of two aromatic rings in new compound series **2** and **3**, and the introduction of sp^3 structures by way of a cyclohexyl or piperidyl group, has resulted in the breakup of the flat,

Table 1. In Vitro Activity of PDE4 Inhibitors[a,b]

Compounds	Compound, R	hPDE4A IC_{50} (nM)	hPDE4B IC_{50} (nM)	hPDE4D IC_{50} (nM)	hPBMC TNFα release[c] IC_{50} (nM)	Thermo-dynamic aqueous solubility[e] (g/L)	Log PAMPA[f] (pH6.8)
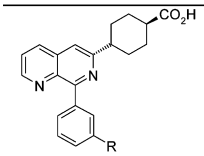	**2a,** SMe	27 ±8	17 ±6	6 ±1	19 ±3	1.1	-3.9
	2b, CN	160 ±53	93 ±23	41 ±20	53 ±24	0.43	-4.0
	2d, F	123 ±9	34 ±6	32 ±10	126 ±60	0.92	-3.7
	2e, OCF_3	107 ±54	43 ±7	24 ±2	52 ±12	0.006	-3.9
	2f, OMe	242 ±41	156 ±16	64 ±22	151 ±28	0.15	-3.8
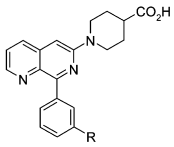	**3a,** SMe	587 ±83	1333	51 ±12	n.d.	0.378	n.d.
	3b, CN	271 ±95	168 ±25	19 ±6	851 ±205	>4	-4.2
	3c, Cl	364 ±208	187	30 ±23	541 ±158	0.14	-4.2
	3d, F	587 ±83	1333	51 ±12	769 ±326	>4	-4.0
	3e, OCF_3	371	225	30	n.d.	1.95	-4.3
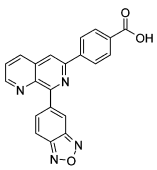	**3f,** OMe	537 ±191	615	45 ±20	1930 ±576	>1	-4.0
	4	602 ±25	34 ±0.5	1.5 ±0.1	67.6 ±1.0	0.002	-4.7

[a]The data represent the mean of at least two separate experiments, each performed in duplicate. [b]Error limits represent standard errors of the mean (SEM) and are shown for those experiments performed at least n = 3 times. [c]TNF-α release measured after stimulation with LPS. [d]n.d. = not determined. [e]Measured at pH6.8. [f]Parallel artificial membrane permeability assay. For method, see ref 17.

dx.doi.org/10.1021/jm300459a | J. Med. Chem. 2012, 55, 7472−7479

Table 2. Pharmacokinetic Parameters of PDE4 Inhibitors in the Rat[a]

	iv V_{ss} (L/kg)	iv Cl (mL/min/kg)	po C_{max} (uM)	po T_{max} (min)	po AUC_{tot} (μM·min)	po $T_{1/2}$ (h)	F (%)
2b[b]	0.25 ± 0.06	0.22 ± 0.1	8.3 ± 1.4	1500 ± 990	112900 ± 42700	193 ± 5	92 ± 18
2d[c]	0.09 (n = 2)	0.64 (n = 2)	4.6 ± 1.0	200.0 ± 51.8	4408 ± 799.0	9 ± 1	52 ± 9
2e[d]	0.36 (n = 2)	0.65 (n = 2)	3.6 ± 0.5	445.0 ± 200.9	5039 ± 849	29 ± 18	107 ± 14
3b[e]	0.72 (n = 2)	1.16 (n = 2)	2.8 ± 0.6	129.0 ± 37.2	2768 ± 566	23 ± 5	158 ± 32
3d[f]	0.24 (n = 2)	2.07 (n = 2)	4.82 ± 0.97	172.5 ± 104.2	3919 ± 1655	17 ± 6	70 ± 12
3e[g]	0.25 ± 0.02	0.98 ± 0.09	4.49 ± 0.51	172.50 ± 48.34	3267 ± 361	7 ± 1	149 ± 17
4	0.37 ± 0.03	2.34 ± 0.39	2.4 ± 1.4	210 ± 87	523 ± 140	12 ± 7	8 ± 3

[a]Error limits are shown as ± SEM where $n \geq 3$. [b]Compound dosed as the potassium salt. Vehicle (iv and po): PBS to 4.2 μM/mL dosed at 4.2 μmol/kg. [c]Compound dosed as the potassium salt. Vehicle (iv and po): PBS to 2.1 μM/mL dosed at 2.1 μmol/kg. [d]Compound dosed as the potassium salt. Vehicle: iv, PBS to 1.05 μmol/mL dosed at 1.05 μ mol/kg; po, PBS to 2.1 μmol/mL dosed at 2.1 μmol/kg. [e]Vehicle: iv, 25/75 PEG200/PBS to 1.05 μmol/mL dosed at 1.05 μmol/kg; po, 25/75 PEG200/PBS to 2.1 μmol/mL dosed at 2.1 μmol/kg. [f]Compound dosed as the sodium salt. Vehicle: iv, 25/75 PEG200/PBS to 2.1 μmol/mL dosed at 2.1 μmol/kg; po, 25/75 PEG200/PBS to 4.2 μmol/mL dosed at 4.2 μmol/kg. [g]Compound dosed as the sodium salt. Vehicle: iv, PBS to 1.05 μmol/mL dosed at 1.05 μmol/kg; po, PBS to 2.1 μmol/mL dosed at 2.1 μmol/kg.

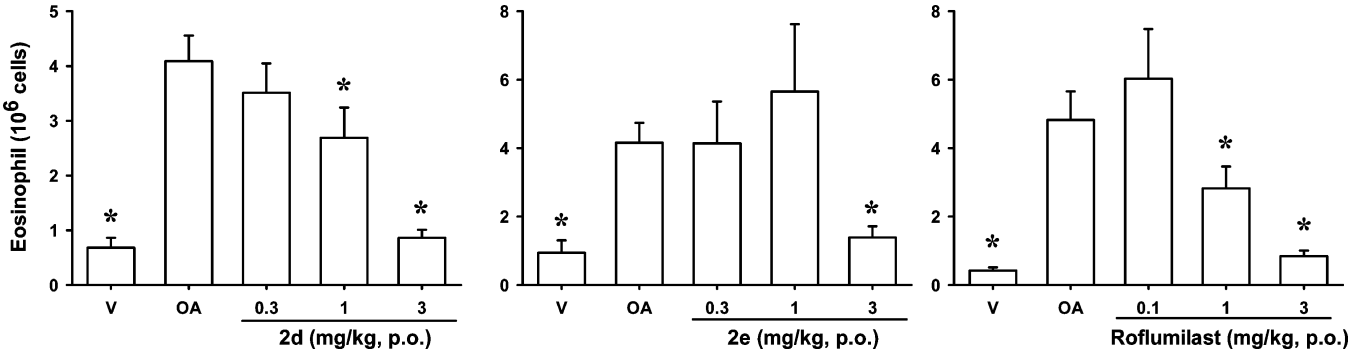

Figure 3. Effects of compounds **2d**, **2e**, and roflumilast on the pulmonary inflammatory response in the airways measured in samples of BAL fluid recovered 24 h after antigen challenge in actively sensitized brown Norway rats. Compounds or vehicle (PEG200:saline 1:1) were given orally 2 h prior to antigen challenge. V = challenge with saline; OA = challenge with ovalbumin. Results are expressed as mean values ± SEM of 5−10 animals per group. *$p < 0.05$ indicates significant difference by comparison with vehicle-treated and OA challenged animals.

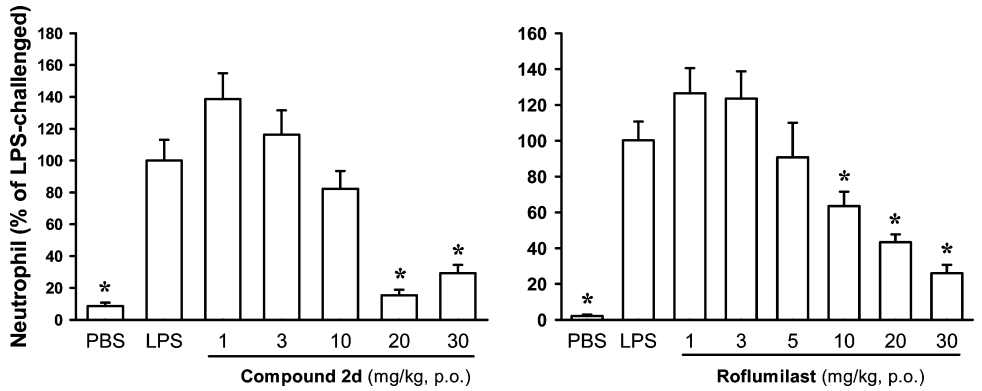

Figure 4. Effect of **2d** and roflumilast on inhibition of LPS-induced lung inflammation in mice. One hour before the LPS challenge, mice were treated via the oral route with vehicle, PEG200:saline 1:1 (LPS) or increasing doses of **2d** or roflumilast (1−30 mg/kg). As a control, a group of animals was treated with vehicle and challenged with PBS (PBS). Animals were killed at 3 h postchallenge. Results are from two experiments and are expressed as individual data and means (horizontal bars) of 6−15 mice per group. Significance indicated by * ($p < 0.05$) was determined using a Mann−Whitney test against the vehicle-treated and LPS-challenged animals (LPS).

lipophilic ABE171 and disrupted the regular, ordered crystal packing structure. In this way, solubility of the new compounds is vastly improved compared to our starting point. Piperidyl series **3** has CLogP at least 1 log unit less than the corresponding cyclohexyl derivative (e.g., CLogP **3d** = 3.198, CLogP **2d** = 4.28), helping the solubility and providing a basic center. The compound which stands out as having surprisingly low solubility is example **2e**. The reason behind this is not entirely clear, however this compound does have a high ClogP at 5.26, and perhaps the electronic effects of the trifluoromethoxy group in this example are such that solubility at this critical pH happens to be low. This generally excellent improvement in solubilities must have been a strong factor in the concomitant improvement in pharmacokinetic properties in the rat. As shown in Table 2, these new compounds typically showed high bioavailability and excellent exposure, in contrast to **4** (Figure 1).

There were no obvious trends in pharmacokinetics when looking across the cyclohexyl or piperidinyl series (compare **2b** with **3b** and **2d** with **3d**). For example, although the half-life of

dx.doi.org/10.1021/jm300459a | J. Med. Chem. 2012, 55, 7472−7479

2b was exceptionally long, and this was reduced by going to the piperidinyl derivative **3b**, there was no reduction in half-life of **3d** compared to **2d**.

Given the excellent in vitro affinity of the PDE4 inhibitors described, it was decided to evaluate selected compounds further in in vivo models of disease.

Effect of PDE4 Inhibitors on the Pulmonary Inflammatory Response in Sensitized Brown Norway (BN) Rats Following Challenge with Inhaled Ovalbumin (OA). Given the data so far on the PDE4 inhibitors, several compounds were selected for in vivo efficacy studies. The OA challenge of actively sensitized BN rats results in a marked increase in eosinophil numbers in bronchoalveolar lavage (BAL) fluid, obtained 24 h following antigen exposure. This model is a well characterized and recognized model for asthma.[12] As shown in Figure 3, oral administration of compounds **2d** and **2e** (0.3, 1, and 3 mg/kg) given 2 h prior to antigen challenge induced dose-dependent inhibition of the numbers of eosinophils present in BAL fluid obtained from actively sensitized BN rats, 24 h after OA challenge. The ED_{50} values against eosinophilia were estimated at approximately 1.2 and 2 mg/kg for compounds **2d** and **2e**, respectively. The known PDE4 inhibitor roflumilast was used as a benchmark in this experiment and seen to have ED_{50} = 0.74 mg/kg.

Inhibition of Lipopolysaccharide (LPS)-Induced Lung Inflammation in Mice. COPD is characterized by an increase in the activation of and/or numbers of macrophages and neutrophils Therefore, it was important to test compounds in a macrophage-dependent model. To do so, we used the LPS-induced lung inflammation model in BALB/c mice, which has been shown to be dependent upon macrophage activation.[13] When given orally, one hour before the LPS challenge, **2d** inhibited neutrophil influx into the BAL fluid with an ED_{50} value of 11.2 ± 1.9 mg/kg. Roflumilast was as potent as compound **2d**, with an ED_{50} value of 12.4 ± 2.9 mg/kg (Figure 4).

The potent activity of the PDE4 inhibitors in attenuating both ovalbumin- and LPS-driven lung inflammation in these experiments is supportive of their having therapeutic potential in asthma and COPD.

Effect of PDE4 Inhibitors in a Ferret Model of Emesis. One of the observed side effects of PDE4 inhibitors in the clinic is their potential to cause nausea and emesis at therapeutic doses. The aim of this study was to assess the emetic potential of our PDE4 inhibitors in a ferret model, the details of which have been described.[14] Roflumilast, currently the most advanced PDE4 inhibitor, was used as the internal standard and compared against compounds **2d** and **2e** (Figure 5).

Among the compounds used, **2e** showed the most promising profile because no emesis was observed at all the doses tested, while roflumilast was shown to be the most emetic agent. Compound **2e** has a similar level of efficacy in a rodent model of inflammation as **2d**. An impression of the relative therapeutic index of the compounds can be gained by examining the extent of emesis at doses concomitant with ED_{50} values in our rat models (albeit there is a species difference). In the rat OA model, the respective ED_{50}s are: **2d** = 1.2 mg/kg, **2e** = 2 mg/kg, roflumilast = 0.74 mg/kg; it may be seen from the graph in Figure 5 that the degree of emesis observed at these doses is less for **2d** compared to roflumilast. In addition, the pharmacokinetic properties of the compounds were examined after oral dosing to investigate whether the degree of emesis was related to exposure (Table 3).

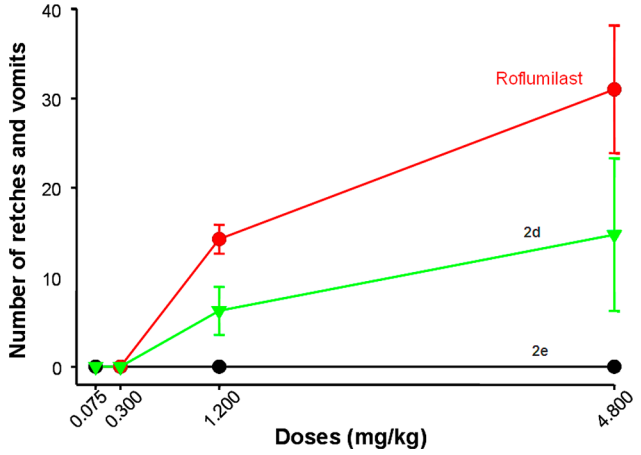

Figure 5. Effect of PDE4 inhibitors in a ferret model of emesis. Compounds were given orally, in a cumulative fashion, every 4 h in PEG200/saline (1/1) and animals observed for signs of emesis. Data are expressed as mean ± SEM of 4–8 ferrets.

As can be seen from Table 3, the maximum concentration and area under the curve indicate good absorption and exposure of compounds **2d** and **2e**. The emetic events occurred at the time when there was maximum concentration of **2d**, however, there was no distinction in the T_{max} between individual animals that did or did not exhibit emesis. The half-life did not appear to be affected by the emetic episodes noted, although the area under the curve (extrapolated) was lower for individual animals that exhibited emesis. No plasma levels were detected for roflumilast or for its possible *N*-oxide metabolite. Possible explanations could be that in the ferret roflumilast is metabolized quickly to a metabolite other than the *N*-oxide or that roflumilast is not absorbed to a great extent. However, animals did show emetic events with a very low systemic exposure of this compound.

It is surprising and of great interest that compound **2e** did not show any emesis in the ferret model despite high systemic exposure. There was no obvious rationale as to why this was the case; certainly, the PDE4 receptor subtype profile is very similar between **2d** and **2e** (although only the human isorforms were tested), as is the ferret pharmacokinetic profile. Other possibilities could be differences in plasma protein binding between the two compounds and differences in brain penetration; however, these parameters were not measured in the ferret.

The aim of this project was to take an established PDE4 inhibitor with good activity on target and to improve the pharmacokinetic and solubility profile in order to produce a developable drug candidate. We have shown that through targeted chemical modifications it is possible to improve the physicochemical properties of molecules while retaining potency on target, resulting in more "drug-like" and pharmaceutically developable compounds. A series of 1,7-naphthyridines has been presented, all of which had excellent pharmacological and physicochemical profiles. Focusing on compounds with the best pharmacokinetics and in vivo activity, we progressed two compounds to the ferret model of emesis, benchmarked against known PDE4 inhibitor roflumilast. In this model, a significant disparity was seen between the emetic potential of two very closely related compounds (**2d** and **2e**), although both could be reasoned to have a better therapeutic window than roflumilast (lower emesis seen at pharmacolog-

dx.doi.org/10.1021/jm300459a | *J. Med. Chem.* 2012, 55, 7472–7479

Table 3. Pharmacokinetic Parameters of PDE4 Inhibitors in the Ferret[a]

compd	C_{max} (μM)	T_{max} (min)	AUC_{tot} (μM·min)	T1/2 (min)
2d[b]	12.3 ± 6.0	90.0 ± 34.6	3560 ± 1690	192 ± 37
2e[c]	10.5 ± 12.8	105.0 ± 30.0	2980 ± 3460	112 ± 83
roflumilast[d]	not detected[e]	not detected	not detected	not detected

[a]Error limits are shown as ± SEM. [b]Formulated as solution in PEG200/saline (50/50, v/v) for intragastric administration at 3.42 μmol/kg. [c]Formulated as solution in PEG200/saline (50/50, v/v) for intragastric administration at 3.42 μmol/kg. [d]Formulated as solution in PEG200/saline (50/50, v/v) for intragastric administration at 2.98 μmol/kg. [e]No plasma levels were detected for roflumilast or for its possible *N*-oxide metabolite (limits of detection were 0.5 and <0.02 μM, respectively).

ically equivalent doses and much higher levels of systemic exposure).

Compounds **2d** and **2e** were selected as potential clinical candidates and were profiled through further preclinical assays. Although compound **2e** appeared by far the better candidate based on the ferret model data, it was felt that emesis as a side effect was less important than other toxicological readouts associated with PDE4 inhibitors such as vasculitis.[2] During a two-week toxicology study in the rat, again using roflumilast as a benchmark, it was found that based on the histopathological assessment of selected organs at the dose group of 2 mg/kg, compound **2d** showed a better toxicological profile compared to **2e** and roflumilast, despite similar doses of the compounds resulting in much higher exposure to **2d** as compared to roflumilast (or its *N*-oxide metabolite). Thus it was interesting to note that there appeared to be no correlation between emetic potential of the compounds in the ferret and toxicological profile in the rat.

CONCLUSION

We have demonstrated that it is possible to take a lead compound with poor solubility and pharmacokinetic profile and to reintroduce solubility based on rational design, in turn achieving an improved pharmacokinetic response. Reproducible and predictable ADME properties are likely to be important in the case of a trial drug acting on a target known to give a low therapeutic window such as PDE4.

In this program, we developed a number of PDE4 inhibitors with in vivo activity, however, the side effect profile proved to be difficult to predict or explain based on any measured physicochemical or biological parameter. Thus, a pragmatic decision was taken to progress the overall most promising compound, particularly looking at the in vivo toxicology in selected organs rather than just at acute emesis. On the basis of these experiments, compound **2d** was chosen for further advancement, and a large scale synthesis developed.[15] The compound was selected for profiling in Ph1 clinical trials in humans, the results of which will be reported in future publications.

EXPERIMENTAL SECTION

All ^{1}H NMR spectra were obtained on either a Bruker AV400 or a Bruker DRX500 spectrometer operating at 400 and 500 MHz for proton, respectively, both at 298K. The AV400 is equipped with a 5 mm inverse 1H/13C dual probe, the DRX500 with a 5 mm BBO probe. Both instruments are operating under Bruker Topspin software. Typical acquisition parameters: spectral width 16 ppm, pulse width of 33°, and data size 64k points. Chemical shifts are reported in values relative to the residual solvent signal (dimethylsulfoxide), and coupling constants are reported in hertz. ^{13}C NMR experiments were carried out on the Bruker AV400 and DRX500 instruments operating at 100 and 125 MHz, respectively, also at 298K. Typical acquisition parameters were a sweep width of 30 kHz, acquisition time of 1.08 s, pulse width of 33°, and data size of 64K points. Again, chemical shifts are reported in ppm relative to the residual solvent resonances.

All final compounds were purified to >95% purity as determined by high performance liquid chromatography (HPLC) with UV detection at 254 and 220 nm and ELSD, using Acquity/Waters SQD LCMS instruments. Low resolution mass spectrometry (MS) data were obtained using a Waters SQD single quadrupole mass spectrometer operating in electrospray ionization (ESI) mode (positive or negative). The following methods were used:

(1) Column: Acquity CSH C18, 100 mm × 2.1 mm, 1.7 μ. A = water + 0.1% formic acid A, B = MeCN + 0.1% TFA. Gradient, 0−8 min 2−98%B, 8−9 min 98%B, 9−9.1 min 98−2%B. Flow rate, 0.7 mL/min

(2) Column: Acquity CSH C18, 100 mm × 2.1 mm, 1.7 μ. A = water + 0.1% ammonia, B = MeCN + 0.1% ammonia. Gradient, 0−8 min 2−98%B, 8−9 min 98%B, 9−9.1 min 98−2%B. Flow rate, 0.7 mL/min

Chemistry. The general procedure for the preparation of 8-aryl-1,7-naphthyridin-6-yltrifluoromethane sulfonate derivatives **1**, including **1b** and **1c**, has been previously described[16] and is followed for the variants in this disclosure. The characterization of representative new compounds is given below and in the Supporting Information:

*8-(3-Fluorophenyl)-1,7-naphthyridin-6-yl trifluoromethanesulfonate (**1d**).* ^{1}H NMR (500 MHz, DMSO-d_6) δ 9.22 (dd, J = 4.1, 1.8 Hz, 1H), 8.65 (dd, J = 8.5, 1.8 Hz, 1H), 8.27 (s, 1H), 8.03 (ddd, J = 8.4, 1.7, 1.0 Hz, 1H), 8.01 (ddd, J = 10.6, 2.7, 1.7 Hz, 1H), 7.95 (dd, J = 8.5, 4.1 Hz, 1H), 7.64 (ddd, J = 8.4, 8.4, 6.2 Hz, 1H), 7.43 (dddd, J = 8.4, 8.4, 2.7, 1.0 Hz, 1H). ^{13}C NMR (126 MHz, DMSO-d_6) δ 161.5 (d, J = 242.5 Hz), 156.8 (d, J = 2.6 Hz), 153.5, 149.9, 140.5, 138.2 (d, J = 8.3 Hz), 136.3, 135.5, 130.0 (d, J = 8.2 Hz), 127.2 (d, J = 2.7 Hz), 126.5, 118.3 (q, J = 321.1 Hz), 118.0 (d, J = 23.7 Hz), 116.8 (d, J = 20.8 Hz), 111.6.

4-Iodocyclohexanecarboxylic Acid Ethyl Ester. To a cold (0 °C) stirred solution of 4-hydroxycyclohexanecarboxylic acid ethyl ester (1.0 g, 5.80 mmol) in 1:2 dichloromethane:carbontetrachloride (52 mL) was added triphenylphosphine (1.82 g, 6.96 mmol), imidazole (473 mg, 6.96 mmol), and iodine (1.79 g, 7.08 mmol). The mixture was allowed to warm to room temperature and stirred overnight. The reaction was quenched by the addition of saturated sodium thiosulfate (ca. 50 mL) and stirred until the solution became clear. The layers were separated, and the aqueous layer was extracted with dichloromethane (3 × 30 mL). The combined organic phases were washed with sodium thiosulfate (30 mL) and brine (30 mL), dried with anhydrous $MgSO_4$, filtered, and evaporated at reduced pressure to an oily solid. Purification was by dry flash chromatography, using Keiselgel 15−40 grade silica, eluting with 3% ethyl acetate/isohexane to yield 4-iodo-cyclohexanecarboxylic acid ethyl ester as a clear colorless oil (801 mg, 49%).

Isomer 1: ^{1}H NMR (400 MHz, DMSO-d_6) δ 4.81 (m, 1H), 4.07 (q, J = 7.1 Hz, 2H), 2.47 (m, 1H), 1.96 (m, 1H), 1.76 (m, 1H), 1.75 (m, 1H), 1.73 (m, 1H), 1.18 (q, J = 7.1 Hz, 3H). ^{13}C NMR (100 MHz, DMSO-d_6) δ 174.2, 59.8, 40.4, 35.8, 35.2, 25.8, 14.1.

Isomer 2: ^{1}H NMR (400 MHz, DMSO-d_6) δ 4.30 (dddd, J = 11.5, 11.5, 3.9, 3.9 Hz, 1H), 4.03 (q, J = 7.1 Hz, 2H), 2.41 (dddd, J = 11.5, 11.5, 3.8, 3.8 Hz, 1H), 2.29 (m, 1H), 1.94 (m, 1H), 1.74 (m, 1H), 1.47 (m, 1H), 1.15 (q, J = 7.1 Hz, 3H). ^{13}C NMR (100 MHz, DMSO-d_6) δ 174.5, 59.8, 40.4, 38.3, 30.3, 30.2, 14.0.

dx.doi.org/10.1021/jm300459a | J. Med. Chem. 2012, 55, 7472−7479

*General Procedure for the Preparation of 4-((8-Aryl)-1,7-naphthyridin-6-yl)cyclohexanecarboxylic Acid Derivatives **2a–2f**.* A flask was charged with activated zinc dust (742 mg, 11.13 mmol), THF (1.80 mL), and 1,2-dibromoethane (25 μL, 0.284 mmol). The suspension was heated to reflux for 3 min and then allowed to cool before trimethylsilyl chloride (29 μL, 0.227 mmol) was added. The mixture was stirred for 15 min, then 4-iodocyclohexanecarboxylic acid ethyl ester (1.60 g, 5.67 mmol) was added and the mixture stirred at 35 °C for 1.5 h. A second flask was charged with Pd-(dibenzylideneacetone)$_2$ (101 mg, 0.176 mmol), 1,1′-bis-(diphenylphosphino)ferrocene (98 mg, 0.176 mmol), *N*-methylpyrrolidinone (NMP) (3 mL):THF (1 mL), tetrabutylammonium iodide (2.79 g, 7.56 mmol), and the appropriate 8-(3-'R'-phenyl)-1,7-naphthyridin-6-yl trifluoromethanesulfonate (956 mg, 2.52 mmol), and the contents were added to the first flask at 35 °C. The reaction mixture was stirred for 2 h, then quenched by the addition of water (15 mL) and stirred for 10 min. Ethyl acetate (40 mL) was then added and stirred for 5 min. The layers were separated, and the organic layer was washed with 5% citric acid (25 mL), water (2 × 25 mL), and brine (40 mL), dried with anhydrous MgSO4, filtered, and evaporated to a brown viscous oil. Purification was by dry flash chromatography using 15–40 grade Keiselgel silica, eluting with 30% ethyl acetate/iso-hexane to yield the [1,7]-naphthyridin-6-yl-cyclohexanecarboxylic acid ethyl ester as an orange gum.

The esters were hydrolyzed to give the final compounds by the following general procedure:

Aqueous lithium hydroxide (1M, 24.3 mL, 24.3 mmol) was added to a solution of the appropriate [1,7]-naphthyridin-6-yl-cyclohexanecarboxylic acid ethyl ester (12.14 mmol) in THF/methanol (40 mL:20 mL) and stirred at room temperature overnight. The organic solvents were removed by evaporation, then the aqueous residue diluted with water and basified to pH 9 with 1 M KOH. The aqueous layer was then washed with ethyl acetate (3×). The aqueous layer was acidified to pH 4 with 1 M HCl to give a white precipitate, which was extracted into ethyl acetate. The ethyl acetate layer was then dried over sodium sulfate, filtered, and concentrated to yield the desired product as a yellow foam. If necessary, further trituration with 1 M HCl yields the product as a pale-yellow powder.

*4-(8-(3-Fluorophenyl)-1,7-naphthyridin-6-yl)-cyclohexanecarboxylic Acid (**2d**).* ^{1}H NMR (500 MHz, DMSO-d_6) δ 12.08 (s, 1H), 9.01 (dd, J = 4.1, 1.9 Hz, 1H), 8.43 (dd, J = 8.3, 1.9 Hz, 1H), 7.99 (ddd, J = 8.0, 1.3, 1.3 Hz, 1H), 7.95 (ddd, J = 10.8, 2.6, 1.3 Hz, 1H), 7.76 (dd, J = 8.3, 4.1 Hz, 1H), 7.76 (s, 1H), 7.56 (ddd, J = 8.0, 8.0, 6.1 Hz, 1H), 7.33 (dddd, J = 8.9, 8.0, 2.6, 1.3 Hz, 1H), 2.88 (dddd, J = 11.9, 11.9, 3.3, 3.3 Hz, 1H), 2.31 (dddd, J = 12.1, 12.1, 3.3, 3.3 Hz, 1H), 2.10 (m, 2H), 2.07 (m, 2H) 1.69 (m, 2H), 1.54 (m, 2H). ^{13}C NMR (126 MHz, DMSO-d_6) δ 176.7, 161.5 (d, J = 241.8 Hz), 158.6, 156.0 (d, J = 2.4 Hz), 151.2, 140.7 (d, J = 8.2 Hz), 139.4, 135.5, 132.5, 129.5 (d, J = 8.3 Hz), 127.1 (d, J = 2.4 Hz), 125.2, 117.7 (d, J = 23.1 Hz), 116.4, 115.4 (d, J = 21.1 Hz), 44.3, 42.1, 31.4, 28.7.

*4-(8-(3-(Trifluoromethoxy)phenyl)-1,7-naphthyridin-6-yl)-cyclohexanecarboxylic Acid (**2e**).* ^{1}H NMR (500 MHz, DMSO-d_6) δ 12.09 (s, 1H), 9.00 (dd, J = 4.1, 1.8 Hz, 1H), 8.43 (m, 1H), 8.18 (ddd, J = 8.0, 1.4, 1.4 Hz, 1H), 8.11 (m, 1H), 7.77 (s, 1H), 7.76 (dd, J = 8.3, 4.1 Hz, 1H), 7.66 (dd, J = 8.0, 8.0 Hz, 1H), 7.49 (m, 1H), 2.88 (dddd, J = 11.9, 11.9, 3.3, 3.3 Hz, 1H), 2.30 (dddd, J = 12.1, 12.1, 3.3, 3.3 Hz, 1H), 2.10 (m, 2H), 2.07 (m, 2H), 1.68 (m, 2H), 1.54 (m, 2H). ^{13}C NMR (126 MHz, DMSO-d_6) δ 176.7, 158.6, 155.6, 151.3, 147.8 (q, J = 1.8 Hz), 140.6, 139.4, 135.5, 132.5, 130.1, 129.5, 125.3, 123.3, 121.0, 120.2 (q, J = 255.9 Hz), 116.6, 44.3, 42.1, 31.4, 28.7.

*General Procedure for the Preparation of 1-((8-Aryl)-1,7-naphthyridin-6-yl)piperidine-4-carboxylic Acid Derivatives **3a–3f**.* The appropriate 8-(3-'R'-phenyl)-1,7-naphthyridin-6-yltrifluoromethanesulfonate (0.53 mmol) was dissolved in DMSO (1.2 mL) with the appropriate amine (l.24 mmol) and the mixture heated at 60 °C for 2 days or until complete by high performance liquid chromatography (HPLC) analysis. After cooling, ethyl acetate was added to the mixture, which was washed four times with brine. The organic layer was dried over sodium sulfate and concentrated. Purification by column chromatography, typically eluting with 25% ethyl acetate in hexane, yielded the desired product as a powder.

*1-(8-(3-Fluorophenyl)-1,7-naphthyridin-6-yl)piperidine-4-carboxylic Acid (**3d**).* ^{1}H NMR (500 MHz, DMSO-d_6) δ 8.63 (dd, J = 4.0, 1.8 Hz, 1H), 8.11 (dd, J = 8.5, 1.8 Hz, 1H), 7.97 (ddd, J = 8.0, 1.3, 1.3 Hz, 1H), 7.94 (ddd, J = 10.8, 2.6, 1.3 Hz, 1H), 7.53 (ddd, J = 8.0, 8.0. 6.1 Hz, 1H), 7.49 (dd, J = 8.5, 4.0 Hz, 1H), 7.29 (dddd, J = 8.9, 8.0, 2.6, 1.3 Hz, 1H), 7.01 (s, 1H), 4.25 (m, 2H), 2.99 (m, 2H), 2.07 (dddd, J = 10.5, 10.5, 3.3, 3.3 Hz, 1H), 1.84 (m, 2H), 1.57 (m, 2H). ^{13}C NMR (126 MHz, DMSO-d_6) δ 176.8, 161.5 (d, J = 241.8 Hz), 154.9, 154.6 (d, J = 2.6 Hz), 147.2, 140.9 (d, J = 8.2 Hz), 135.1, 135.1, 133.9, 129.4 (d, J = 8.2 Hz), 126.9 (d, J = 2.4 Hz), 124.7, 117.5 (d, J = 22.8 Hz), 115.2 (d, J = 21.1 Hz), 98.0, 45.5, 43.9, 28.9.

PDE4 in Vitro Assays. The PDE4 isoform assays were based on Amersham Pharmacia Biotech Scintillation Proximity Assay (SPA) technology. The enzyme was diluted with enzyme dilution buffer (10 mM Tris-HCI, pH7.5 containing 1 mM EDTA) in order to obtain between 10 and 30% total substrate hydrolysis during the assay. The enzymatic reaction was started by adding 10 μL of diluted enzyme to 80 μL of substrate (0.1 μCi [3H]-cAMP, 1 μM cAMP) and 10 μL of inhibitor solution in a 96-well microtiter plate. After 30–60 min incubation at room temperature, the reaction was stopped by adding 50 μL of PDE SPA beads (20 mg/mL). After 30 min, the plate was centrifuged (3000*g*, 10 min) and counted (Packard TopCount). Inhibitor stock solutions were prepared in 100% dimethylsulfoxide (DMSO) and diluted with DMSO/water to achieve 10 concentrations to cover the range of 0–100% inhibition. The concentration of DMSO is kept constant at 1% (v/v) throughout the assay. The concentration at which 50% inhibition occurs (IC_{50}) was determined from inhibition concentration curves.

hPBMC Activation Assay. Peripheral blood mononuclear cells (PBMC) were isolated from the blood of normal individuals by Ficoll–Hypaque gradient centrifugation (20 min at 800*g*). The interphase was collected, washed twice in PBS, and resuspended in RPMI1640 supplemented with 10% FCS. Cell density was then adjusted to 1 × 10^6 cells/mL. The PBMC suspension (100 μL) was placed in 96-well culture plates, and 50 μL of either medium or compound were added (compound solutions were prepared as above). After a 10 min preincubation, cells were stimulated with LPS (50 μL, 10 ng/mL) for the production of TNF-α. Supernatants were harvested after incubating the plates for 20 h at 37 °C in a humidified incubator with 5% CO_2.

TNF-α was measured by sandwich ELISA using a primary anti-TNF-α monoclonal antibody purchased from Pharmingen (UK). Binding of the secondary antibody was analyzed by stepwise incubation with streptavidin–alkaline phosphatase conjugate (Sigma, UK) and 4-nitrophenylphosphate disodium salts (Sigma, UK).

Optical density was measured at 405 nm, and cytokine concentration was calculated based on the results from serial dilutions of standard recombinant TNF-α. The sensitivity of the cytokine ELISA was approximately 10 pg/mL. The concentration at which 50% inhibition occurs (IC_{50}) was determined from inhibition concentration curves.

■ ASSOCIATED CONTENT

Ⓢ Supporting Information

Experimental results for examples **1a**, **1e**, **1f**, **2a–b**, **2f**, **3a–c**, and **3e–f**. This material is available free of charge via the Internet at http://pubs.acs.org.

■ AUTHOR INFORMATION

Corresponding Author

*Phone: +44 1403 272827. Fax: +44 1403 323 837. E-mail: neil.press@novartis.com.

Notes

The authors declare no competing financial interest.

■ ACKNOWLEDGMENTS

We thank Professor R. J. Naylor, University of Bradford, for performing the ferret emesis experiments.

■ ABBREVIATIONS USED

BAL, bronchoalveolar lavage; BN, brown Norway; PDE4, phosphodiesterase-4; HARBS, high affinity rolipram binding site; OA, ovalbumin; PBMC, peripheral blood mononuclear cell

■ REFERENCES

(1) Dastidar, S. G.; Rajagopal, D.; Ray, A. Therapeutic benefit of PDE4 inhibitors in inflammatory diseases. *Curr. Opin. Invest. Drugs (Thomson Sci.)* **2007**, *8*, 364−372.

(2) Press, N. J.; Banner, K. H. PDE4 inhibitors—a review of the current field. *Prog. Med. Chem.* **2009**, *47*, 37−74.

(3) Boswell-Smith, V.; Spina, D. PDE4 inhibitors as potential therapeutic agents in the treatment of COPD-focus on roflumilast. *Int. J. Chronic Obstruct. Pulm. Dis.* **2007**, *2*, 121−129.

(4) Martin, N.; Reid, P. T. The potential role of phosphodiesterase inhibitors in the management of asthma. *Treat. Respir. Med.* **2006**, *5*, 207−217.

(5) Spina, D. The potential of PDE4 inhibitors in respiratory disease. *Curr. Drug Targets: Inflammation Allergy* **2004**, *3*, 231−236.

(6) Cazzola, M.; Picciolo, S.; Matera, M. G. Roflumilast in chronic obstructive pulmonary disease: evidence from large trials. *Expert Opin. Pharmacother.* **2010**, *11*, 441−449.

(7) (a) Giembycz, M. A. Can the anti-inflammatory potential of PDE4 inhibitors be realized: guarded optimism or wishful thinking? *Br. J. Pharmacol.* **2008**, *155*, 288−290. (b) Chapman, R. W.; House, A; Richard, J; Prelusky, D; Lamca, J; Wang, P; Lundell, D; Wu, P; Ting, P. C.; Lee, J. F.; Aslanian, R; Phillips, J. E. Pharmacology of a potent and selective inhibitor of PDE4 for inhaled administration. *Eur. J. Pharmacol.* **2010**, *643*, 274−281.

(8) Hersperger, R.; Dawson, J.; Mueller, T. Synthesis of 4-(8-benzo[1,2,5]oxadiazol-5-yl-[1,7]naphthyridine-6-yl)-benzoic acid: a potent and selective phosphodiesterase type 4D inhibitor. *Bioorg. Med. Chem. Lett.* **2002**, *12*, 233−235.

(9) Trifilieff, A.; Wyss, D.; Walker, C.; Mazzoni, L.; Hersperger, R. Pharmacological profile of a novel phosphodiesterase 4 inhibitor, 4-(8-benzo[1,2,5]oxadiazol-5-yl-[1,7]naphthyridin-6-yl)benzoic acid (**4**), a 1,7-naphthyridine derivative, with anti-inflammatory activities. *J. Pharmacol. Exp. Ther.* **2002**, *301*, 241−248.

(10) Tigani, B.; Cannet, C.; Zurbruegg, S.; Schaeublin, E.; Mazzoni, L.; Fozard, J. R.; Beckmann, N. Resolution of the oedema associated with allergic pulmonary inflammation in rats assessed noninvasively by magnetic resonance imaging. *Br. J. Pharmacol.* **2003**, *140*, 239−246.

(11) Crystallographic data (excluding structure factors) for the structure in this paper have been deposited with the Cambridge Crystallographic Data Centre as supplementary publication numbers CCDC 873054. Copies of the data can be obtained, free of charge, on application to CCDC, 12 Union Road, Cambridge CB2 1EZ, UK (fax: +44 (0)1223−336033 or e-mail: deposit@ccdc.cam.ac.uk).

(12) Renzi, P. M.; Olivenstein, R.; Martin, J. G. Inflammatory cell populations in the airways and parenchyma after antigen challenge in the rat. *Am. Rev. Respir. Dis.* **1993**, *147*, 967−974.

(13) Goncalves, d. M.; Singer, M.; Vargaftig, B. B.; Chignard, M. Effects of rolipram on cyclic AMP levels in alveolar macrophages and lipopolysaccharide-induced inflammation in mouse lung. *Br. J. Pharmacol.* **1998**, *123*, 631−636.

(14) Costall, B.; Domeney, A. M.; Naylor, R. J.; Tattersall, F. D. Emesis induced by cisplatin in the ferret as a model for the detection of antiemetic drugs. *Neuropharmacology* **1987**, *26*, 1321−1326.

(15) Jiang, X.; Lee, G. T.; Villhauer, E. B.; Prasad, K.; Prashad, M. A Scalable Synthesis of a 1,7-Naphthyridine Derivative, a PDE-4 Inhibitor. *Org. Process Res. Dev.* **2010**, *14*, 883−889.

(16) Hersperger, R; Bray-French, K; Mazzoni, L; Müller, T. Palladium-Catalyzed Cross-Coupling Reactions for the Synthesis of 6,8-Disubstituted 1,7-Naphthyridines: A Novel Class of Potent and Selective Phosphodiesterase Type 4D Inhibitors. *J. Med. Chem.* **2000**, *43* (4), 675−682.

(17) Wohnsland, F.; Faller, B. High-Throughput Permeability pH Profile and High-Throughput Alkane/Water log *P* with Artificial Membranes. *J. Med. Chem.* **2001**, *44* (6), 923−930.